Journal of Ultrafine Grained and Nanostructured Materials
https://jufgnsm.ut.ac.ir
Vol. 57, No.2, December 2024, pp. 135-144
Print ISSN: 2423-6845 Online ISSN: 2423-6837
DOI: 10.22059/jufgnsm.2024.02.04

One-Step Synthesis of PEG-Functionalized Gold Nanoparticles: Impact of Low Precursor Concentrations on Physicochemical Properties

Melbagrace Lapening [a], Rolen Brian Rivera [a,c*], Romnick Unabia [b], Renzo Luis Reazo [a], Jahor Omping [a], Ryan Lumod [a], Archie Ruda [a], Amyzz Ceniza [e], Noel Lito Sayson [a,c], Felmer Latayada [d], Rey Capangpangan [e], Gerard Dumancas [f,g], Arnold Lubguban [h], Roberto Malaluan [h], Ahmad Hosseini-Bandegharae[i,j,k], Gaudencio Petalcorin Jr. [l], and Arnold Alguno[a,m,*]

[a] Research Center for Energy Efficient Materials (RCEEM), Premier Research Institute of Science and Mathematics (PRISM), MSU-Iligan Institute of Technology, 9200 Iligan City, Philippines
[b] IT and Physics Department, College of Natural Sciences and Mathematics, Mindanao State University - General Santos, General Santos City, 9500 South Cotabato, Philippines
[c] Department of Physics, Mindanao State University-Iligan Institute of Technology, 9200 Iligan City, Philippines
[d] Department of Chemistry, Caraga State University, Butuan City 8600, Philippines
[e] Department of Physical Sciences and Mathematics, College of Marine and Allied Sciences, Mindanao State University at Naawan, Naawan 9023, Misamis Oriental, Philippines
[f] Honors College, Henry E. and Shirley T. Frye Hall, Suite 110, North Carolina Agricultural and Technical State University, 1601 East Market Street, Greensboro, NC 27411 USA
[g] Department of Chemistry, New Science Building, North Carolina Agricultural and Technical State University 1601 E. Market Street, Greensboro, NC 27411 USA
[h] Center for Sustainable Polymers, Mindanao State University-Iligan Institute of Technology, Iligan City 9200, Philippines
[i] Faculty of Chemistry, Semnan University, Semnan, Iran
[j] Department of Sustainable Engineering, Saveetha School of Engineering, SIMATS, Chennai-602105, Tamil Nadu, India
[k] Center of Research Impact and Outcome, Chitkara University, Rajpura-140401, Punjab, India
[l] Department of Mathematics and Statistics, Mindanao State University-Iligan Institute of Technology, 9200 Iligan City, Philippines
[m] Department of Materials and Resources Engineering and Technology, Mindanao State University-Iligan Institute of Technology, Iligan City 9200, Philippines

Recieved: 29 August 2024; Accepted: 13 October 2024

**Corresponding authors, Rolen Brian Rivera:* (rolenbrian.rivera@g.msuiit.edu.ph); *Arnold Alguno:* (arnold.alguno@g.msuiit.edu.ph)

ABSTRACT

Polyethylene glycol-capped gold nanoparticles (PEG-AuNPs) are highly promising for biological and medical applications due to their biocompatibility, enhanced stability, and low cytotoxicity. The successful synthesis method presented here was a one-step process where both reduction and functionalization took place simultaneously using lower concentrations of gold precursors. Unlike previous methods that used higher concentrations (> 10 mM) and did not explore varying molar ratios, this study investigates the physicochemical properties of PEG-AuNPs synthesized with precursor concentrations ranging from 0.5 mM to 5 mM. Transmission electron microscopy images revealed an increase in the particle sizes of spherical nanoparticles from 14.5nm to 46.7nm as the precursor concentration increased, consistent with dynamic light scattering measurements. UV-Vis spectroscopy confirmed that spherical nanoparticles were formed having surface plasmon resonance peaks ranging from 520-530 nm. Fourier transform infrared spectroscopy analyses revealed the interactions between PEG ligands and gold nanoparticles where some specific peaks exist around 1632cm^{-1} while the O-H stretching peak shifted from approximately 3400 cm^{-1} to about 3490 cm^{-1}, confirming successful surface modification. Photoluminescence spectroscopy revealed maximum emission particularly observed at the lowest precursor concentration (0.5 mM). Importantly, the synthesized PEG-AuNPs even at the lowest precursor concentration of 0.5mM demonstrated exceptional stability in saline conditions, maintaining dispersion even in the presence of 500 mM NaCl. This one-step synthesis method at reduced precursor concentrations not only enables precise control over the nanoparticles' size and optical properties but also enhances their stability and tunable fluorescence. These findings present a scalable and versatile approach for the tailored synthesis of PEG-AuNPs, making them suitable for advanced biological and medical sensing applications.

Keywords: *Gold nanoparticles, Precursor concentration, One-step synthesis, Polyethylene glycol.*

1. Introduction

The development of efficient and environmentally friendly methods for synthesizing nanoparticles is continuously gaining growing interest over time. Nanomaterials are important due to their distinctive nanoscale properties, including a high surface area, enhanced reactivity, and unique electronic, optical, and mechanical characteristics, which facilitate groundbreaking applications in diverse fields such as targeted drug delivery and advanced biosensing applications. Particular interest is given to these particles as they behave differently from their bulk matter counterpart, giving rise to several applications that are not possible at large scale [1]. Gold nanoparticles have gained substantial attention over other metallic nanomaterials owing to their distinctive localized surface plasmon resonance (LSPR) property, high specificity, and relatively low cytotoxicity [2–4]. These characteristics make them ideal for various applications in biomedicine and biotechnology, such as cancer treatment, diagnostic imaging, drug delivery, and biosensing [5–7]. In addition, the straightforward synthesis procedure of AuNPs confers a considerable advantage compared to alternative nano-engineered materials.

The chemical synthesis of AuNPs encompasses distinct approaches, with the widely accepted method proposed by Turkevich et al. in 1951 [8], which was further refined by Frens in 1973 [9]. This method utilized trisodium citrate as a reducing and capping agent to the gold precursor, successfully producing AuNPs ranging from 15-30 nm with high monodispersity. However, the stability of citrate-reduced AuNPs mainly relies on electrostatic repulsion, which can hardly prevent uncontrolled aggregation in specific environmental conditions. Moreover, the surface chemistry of the resulting colloids is poorly defined, inhibiting the direct functionalization of the nanoparticles. These pose a great challenge in biological and medical applications where stability and biocompatibility are significant considerations. To address these drawbacks, numerous alternative synthesis methods were developed to formulate biocompatible AuNPs. Depending on the reagents used, they vary into several techniques such as plant-based approach [10–11], metabolic reduction [12], and microbial technique [13]. These methods, however, are time-consuming, complicated, and require highly specialized training and equipment.

A simpler alternative approach is proposed using cap citrate-reduced AuNPs with biocompatible compounds such as organic ligands, polysaccharides, polymers, amino acids, etc. [14]. Out of these compounds, poly(ethylene) glycol (PEG), a biodegradable polymer, has been frequently utilized in nanoparticle synthesis as a capping agent due to its biocompatibility and ability to reduce cytotoxicity while at the same time giving improved colloidal stability [15,16]. When adsorbed on the nanoparticle's surface, PEG offers steric hindrance against proximate nanoparticles, preventing uncontrolled coagulation that results in a more stable dispersion [17]. Specifically, gold nanoparticles capped with PEG (PEG-AuNPs) are reported to have the highest drug-loading capacity and less cytotoxicity compared to those capped with other coatings, making them a promising candidate for several biological and medical applications such as targeted and controlled release drug delivery systems, intracellular sensing, and gene therapy [18,19].

In a typical synthesis procedure, PEG-AuNPs are produced in two steps: (i) reduction of the gold precursor with a reducing agent to produce a colloidal solution of AuNPs and (ii) surface modification of the resulting colloids with PEG through ligand exchange and adsorption to the surface of the AuNPs, and this has been the common approach adopted up to the present [20–22]. While widely adopted, this method involves additional steps that increase both the cost and time of production. A more streamlined alternative, the one-step approach, has been previously reported, where reduction and pegylation occur simultaneously in a single reaction vessel using high concentrations of the gold precursor [23–25]. Stiufiuc et al. [24] described a one-step method for synthesizing PEG-AuNPs, utilizing polyethylene glycol (PEG) of varying molecular weights to simultaneously serve as the reducing and stabilizing agents. However, this method is often limited by the high precursor usage and lacks detailed investigations into how varying molar ratios of the precursors—especially at lower concentrations—affect the physicochemical properties of PEG-AuNPs.

Addressing these gaps, our study explores a cost-effective and efficient one-step synthesis method that reduces the precursor concentration while varying the molar ratios of the initial precursors. This approach aims to optimize the synthesis process, reducing production costs while maintaining control over the nanoparticles' characteristics. The as-synthesized PEG-AuNPs were comprehensively characterized using transmission electron microscopy (TEM) and dynamic light scattering (DLS) to evaluate their morphological and colloidal properties. Their optical characteristics were examined through UV-Vis spectroscopy, Fourier transform infrared (FT-IR) spectroscopy, and photoluminescence (PL) spectroscopy. Additionally, the crystal structure of the PEG-AuNPs was elucidated using

X-ray diffraction (XRD). Furthermore, this study also evaluates the colloidal stability of PEG-AuNPs under physiological salt conditions, addressing a key challenge in their practical applications. By investigating this simplified synthesis route, we aim to overcome the limitations of traditional methods and provide a more accessible approach to PEG-AuNP production for broader use in advanced biological and medical sensing applications.

2. Experimental details

2.1. Reagents

Gold (III) chloride hydrate ($HAuCl_4$, 99.995% trace metals basis), polyethylene glycol (PEG, Mw=1000 g/mol), and sodium chloride (NaCl, ACS reagent, ≥99.0%) were purchased from Sigma-Aldrich. Sodium hydroxide (NaOH, Hi-AR™/ACS) was purchased from HiMedia Laboratories. These chemicals were used without further modifications. Milli-Q ultrapure water (18.2 MΩ·cm, Merck KGaA) was utilized in all experimental procedures.

2.2. Instrumentation

UV-Vis absorption spectra of the as-prepared colloids were acquired using a Thermo Scientific GENESYS 10S spectrometer (Thermo-Scientific, Massachusetts, US) with a spectral bandwidth of 1.8 nm. This analysis was conducted within the spectral range spanning from 200 to 1000 nm, with a spectral resolution of 1.0 nm. The morphology, average particle diameter, and microphotographs of the PEG-AuNPs were acquired through a JEM 2100 Plus LaB6 model transmission electron microscope (TEM) equipped with STEM operating at an accelerating voltage of 200 kV. Each sample was carefully deposited onto a 3mm copper grid with formvar/carbon supporting film and allowed to air-dry for 10-15 mins before characterization. The resulting images were then analyzed using Image J software. Dynamic Light Scattering (DLS) measurements were performed using a Nanotrac Wave II Analyzer (Microtrac, Inc., Pennsylvania, USA) to obtain the average hydrodynamic diameter. In this process, a 1 mL sample was introduced into a stationary cell and allowed to run for 60 seconds. FT-IR spectra of dried AuNP samples and pure PEG were recorded using an IRTracer-100 FT-IR spectrophotometer (Shimadzu, Japan) with multi-bound attenuated total reflectance (ATR) accessories, carried out in the spectral range between 4000 cm^{-1} and 400 cm^{-1} with 0.25 cm^{-1} resolution. To prepare the samples, 1 mL of the PEG-capped AuNPs were placed in an Eppendorf tube and centrifuged at 4000 rpm for 10 minutes. Following the removal of the supernatant, a small portion of the precipitates was taken and allowed to air-dry before analysis. Photoluminescence spectroscopy was carried out using a FluoroMax Plus Spectrofluorometer. Without any further enhancement, the samples were analyzed at various excitation wavelengths until maximum intensity was achieved. X-ray diffraction (XRD) analysis was performed using D2 Phase Bruker X-ray diffraction equipment with Cu Kα radiation. All the above-mentioned measurements were performed at room temperature.

2.3. Preparation of PEG-AuNPs

The one-step process in synthesizing PEG-capped AuNPs described in Ref [24] was adopted herein with slight modifications. Briefly, an unmodified aqueous solution of PEG (Mw=1000 g/mol) was dissolved in an Erlenmeyer flask containing 45 mL ultrapure water. Next, NaOH (0.25 M) was carefully mixed to the solution. The mixture was then heated up to 50 °C in a water bath to ensure uniform heating. Upon reaching the temperature, an aqueous chloroauric acid solution was quickly added to the mixture under vigorous mechanical stirring. To achieve varied precursor concentration, the concentration of the chloroauric acid was varied from 0.5 mM, 0.75 mM, 1 mM, 2 mM, 3 mM, 4 mM, and 5 mM. The reaction was allowed to proceed until the temperature reached 80 °C. At this stage, the solution displayed a distinctive wine-red color, indicating the successful formation of PEG-capped gold nanoparticles. The as-synthesized colloids were then cooled to room temperature and subsequently stored to 4 °C prior to further analysis.

2.4. Colloidal stability experiments

The investigation of the as-synthesized PEG-AuNPs under physiological salt conditions was conducted across increasing ionic strength levels by adding an aqueous solution of NaCl at different concentrations. Specifically, 270 uL of PEG-AuNPs samples were dispensed into individual microplate cells, followed by the direct addition of 30 uL NaCl solution. This process was repeated at increasing molarities of NaCl, starting from 10 mM up to 1000 mM and was carried out for all samples. For quantitative analysis, 1800 uL of representative PEG-AuNPs samples were placed in a quartz cuvette then added with 200 uL of NaCl at different molarities. The solution was gently swirled to ensure thorough mixing, then subsequently subjected to UV-vis analysis. The absorbance ratio at 650 nm (A_{650}) and at the sample's corresponding peak (A_{peak}) were recorded in order to quantitatively evaluate the dispersion stability of the as-synthesized PEG-AuNPs.

3. Results and discussion

3.1. Morphological studies

The TEM micrographs of the as-synthesized

PEG-AuNPs were presented in Fig. 1. The results indicate the presence of predominantly spherical gold nanoparticles, which exhibit a uniform coating of PEG molecules. The mean particle size was determined to be about 14.5 nm and 46.7 nm for PEG-AuNPs prepared with 0.5 mM (Fig. 1A) and 4 mM (Fig. 1B) precursor concentration, respectively. The dynamic light scattering measurements, as illustrated in Fig. 2, revealed that the average hydrodynamic diameter of the particles falls within the 20-50 nm range. The difference from the size obtained by TEM accounts the PEG molecules that are adsorbed to the surface of the nanoparticles.

For all samples, the polydispersity index (PDI) did not exceed 0.3 (Table 1) and was even lower than 0.1 for samples synthesized with sub-mM precursor concentrations. These values indicate that the obtained nanoparticles are uniformly distributed with respect to the particle size, which improves as the precursors were below 1 mM. As established in a review [26], PDI values below 0.3 are regarded to be acceptable in several drug delivery applications and are most commonly deemed practical for polymer-based nanoparticles when its value is less than 0.2. This enhanced monodispersity corroborates the feasibility of this synthesis method at even lower precursor concentrations (<1 mM).

3.2. Fourier transform infrared studies

To verify the surface modification of PEG around the gold nanoparticle surface, FT-IR spectroscopy was employed. Fig. 3 shows the transmittance spectra of the as-synthesized PEG-AuNPs and PEG precursor. The peak around 940 cm^{-1} is assigned to the out-of-plane bending of -CH- vibrations. The peak at 1100 cm^{-1} and 1261 cm^{-1} is associated with the C-O-C stretching bands of ether, and the infrared-active C-O stretching vibrations, respectively. The

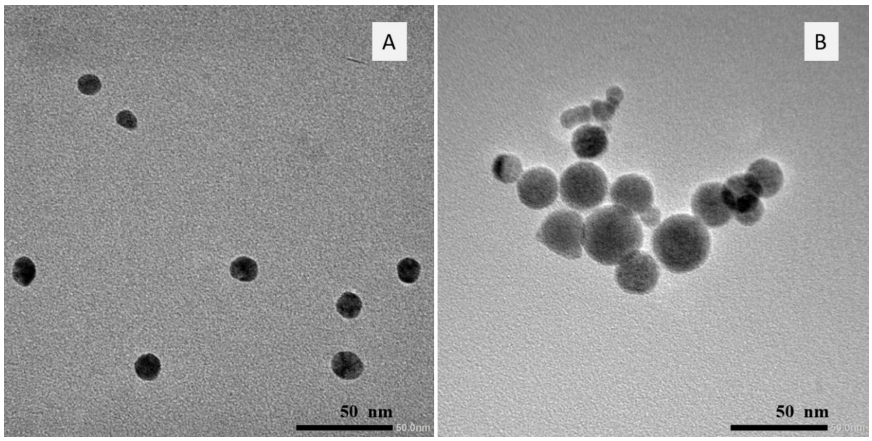

Fig. 1- TEM micrograph of PEG-AuNPs obtained using (A) 0.5 mM and (B) 4 mM chloroauric acid solution showing the impact of low concentration of $HAuCl_4$ on the particle size and morphology of PEG-AuNPs.

Table 1- Absorption maximum, polydispersity index, and pH value of PEG-AuNPs synthesized with varying precursor concentration.

Sample	$HAuCl_4$ Concentration (mM)	Absorption Maximum (nm)	Polydispersity Index (PDI)	pH
A	**0.50**	**536**	**0.087**	**11.03**
B	**0.75**	**526**	**0.084**	**11.17**
C	**1**	**520**	**0.197**	**11.03**
D	**2**	**520**	**0.274**	**10.86**
E	**3**	**521**	**0.271**	**10.21**
F	**4**	**523**	**0.280**	**10.54**
G	**5**	**528**	**0.199**	**10.35**

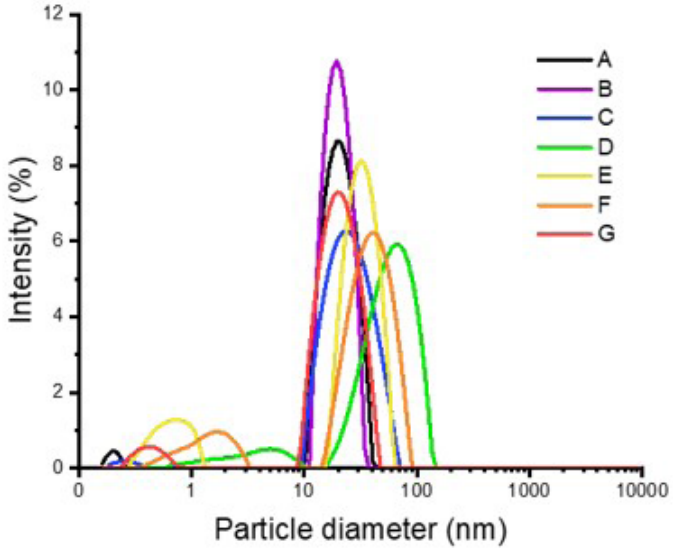

Fig. 2- Average hydrodynamic diameter of PEG-AuNPs with varying concentrations of chloroauric acid solution (0.5 mM, 0.75 mM, 1 mM, 2 mM, 3 mM, 4 mM, and 5 mM labeled A to G, respectively) ranges 20-50 nm with the 0.75 mM $HAuCl_4$ sample exhibiting the most uniform size distribution with PDI of approximately 0.084.

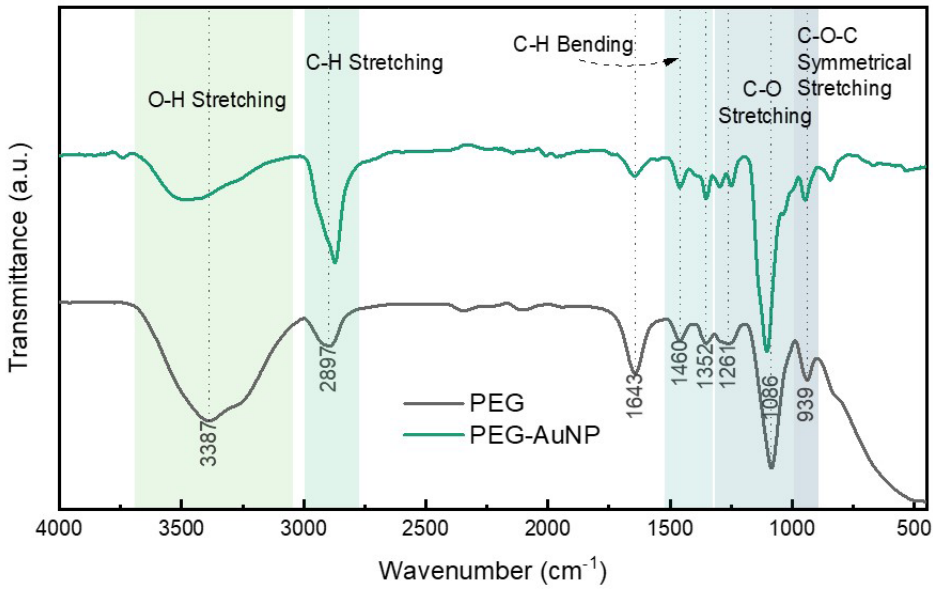

Fig. 3- FT-IR spectra of PEG-AuNPs (green) and pure unmodified PEG solution (gray). The presence of characteristic absorption peaks of pure PEG in the PEG-AuNPs spectrum confirmed its successful attachment to the AuNPs' surface.

presence of methylene C-H stretching and bending vibrations of the –CH_2 group of PEG were observed at 2900 cm^{-1} and 1460 cm^{-1}. In addition, the peak around 3400 cm^{-1} is attributed to the O-H stretching of the terminal hydroxyl group of PEG polymer.

It can be observed that this peak shifted towards 3490 cm^{-1} with increasing intensity upon the formation of PEG-AuNPs [27]. Furthermore, the observed peak at 1645 cm^{-1} of PEG-AuNP spectra was ascribed to the asymmetric stretching of the gold carboxylate unidentate bond which implies the oxidative transformation of PEG terminal alcohol groups into carboxylate entities. This transformation accounts for the negative charge on the surface of gold colloids and their interaction with PEG, further corroborating that PEG functions as both the reducing and stabilizing agent. The presence of these characteristic peaks of PEG precursor in the spectrum of PEG-AuNPs confirms the modification of the surface of the nanoparticles with PEG ligands.

3.3. Optical studies

A narrow and well-defined absorption band was observed at approximately 520 nm (Fig. 4a), which suggest the presence of spherical AuNPs characterized by a uniform size and shape distribution. This characteristic absorption pattern is consistent across all samples except for the lowest concentration (0.5 mM, curve A), where a noticeable shift in the Surface Plasmon Resonance peak occurred, extending to a longer wavelength at around 536 nm. Additionally, a shoulder around 650 nm appeared in the spectrum for this particular sample. The observed spectral changes in the lowest concentration sample may be indicative of several factors. As reported by previous literature [28], this alteration could be attributed to the possibility that the formed colloids have either assumed an anisotropic shape or undergone agglomeration during the characterization process. Photoluminescence spectroscopy revealed an interesting effect of reducing precursor concentration on the optical properties of PEG-AuNPs. As shown in Fig. 4b, the maximum photoluminescence spectra were generated using an excitation wavelength of 500 nm and normalized at the maximum value. It was observed that the PL emission peaks at 751 nm and increases in intensity without undergoing any wavelength shift as the precursor concentration reaches to lower values. Moreover, the maximum emission was particularly observed at the lowest precursor concentration (0.5 mM). This result relates to the dependence of the particle growth on the precursor concentration, as elucidated in previous report [29].

When the precursor concentration is low, the number of elementary gold units necessary to grow the clusters is also low, which, in turn, results in the formation of smaller nanoparticles. Consequently, smaller nanoparticles have larger surface area, which causes multiple reflections and scattering of the photoluminescence excitation beam, thus strengthening the peak intensity of PL emissions [30]. In contrast, when nanoparticles are larger, the peak intensity of PL emission is weaker because the surface area is significantly reduced, diminishing the beam's reflection and scattering. Henceforth, the maximum photoluminescence peak intensity was observed at the lowest precursor concentration (0.5 mM, curve A), with the highest precursor concentration being the lowest in PL emission (5 mM, curve G).

3.4. X-ray Diffraction studies

X-ray diffraction (XRD) analysis of the

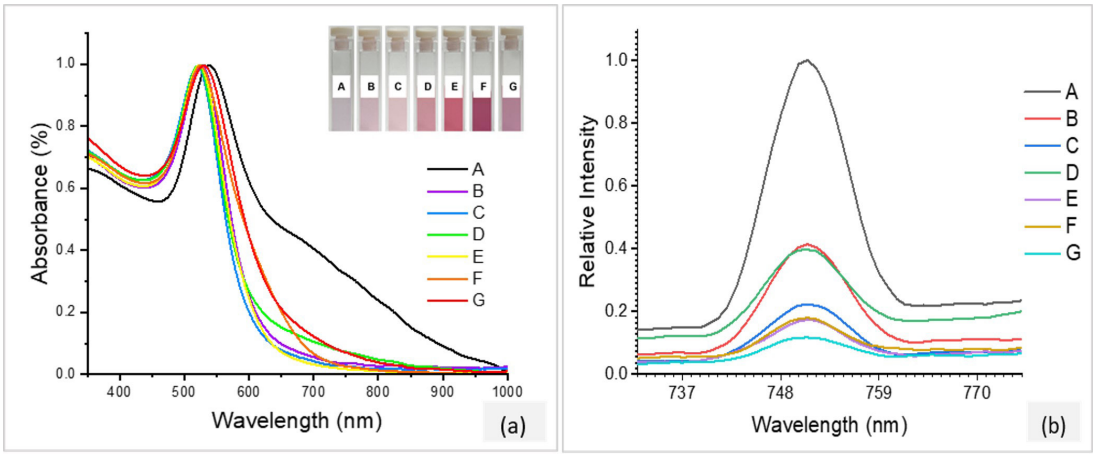

Fig. 4- (a) UV-vis absorption band and (b) photoluminescence emission spectra at an excitation wavelength of 500 nm of PEG-AuNPs obtained via one-step approach using varying $HAuCl_4$ concentration 0.5 mM (A), 0.75 mM (B), 1 mM (C), 2 mM (D), 3 mM (E), 4 mM (F), and 5 mM (G). Inset of (a): actual image of the samples.

synthesized PEG-AuNPs confirms their crystalline structure (Fig. 5). The diffraction peaks are observed at 2θ values of 38.2°, 44.5°, 64.7°, and 77.7°, corresponding to the (111), (200), (220), and (311) planes of the AuNPs. These standard peaks are consistent with the face-centered cubic (FCC) structure of gold, as referenced by JCPDS 65-2870. The dominant peak at 38.1° indicates preferential growth along the (111) plane.

3.5. Colloidal stability of PEG-AuNPs

The stability of the as-synthesized PEG-AuNPs under physiological salt condition was evaluated by introducing varying concentrations of NaCl solution ranging from 10 mM to 1000 mM. Fig. 6 displays the ratio of the colloids' absorbance at 650 nm versus that at the maximum absorption peak of the samples. Notably, at the highest precursor concentration, PEG-AuNPs began to

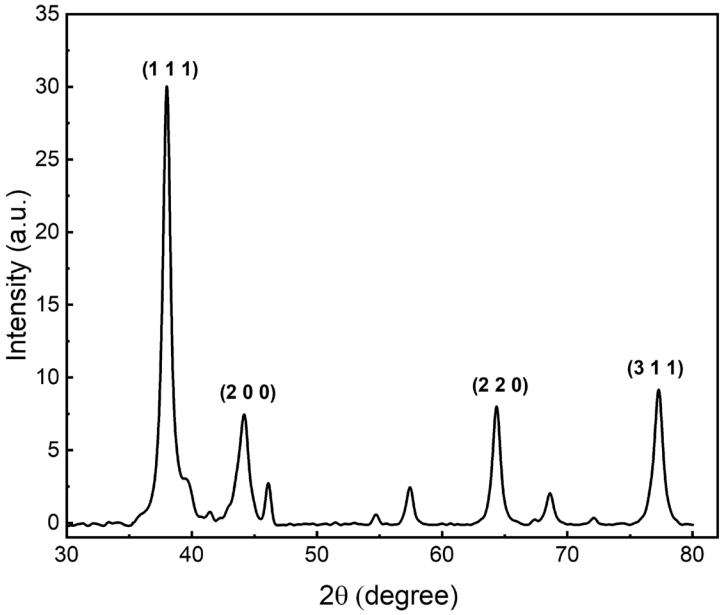

Fig. 5- XRD pattern of PEG-AuNPs synthesized via a one-step method. The crystalline structure is confirmed by four characteristic peaks corresponding to the standard Bragg reflections of a face-centered cubic (FCC) lattice: (111), (200), (220), and (311). The dominant peak at 38.1° indicates preferential growth along the (111) plane.

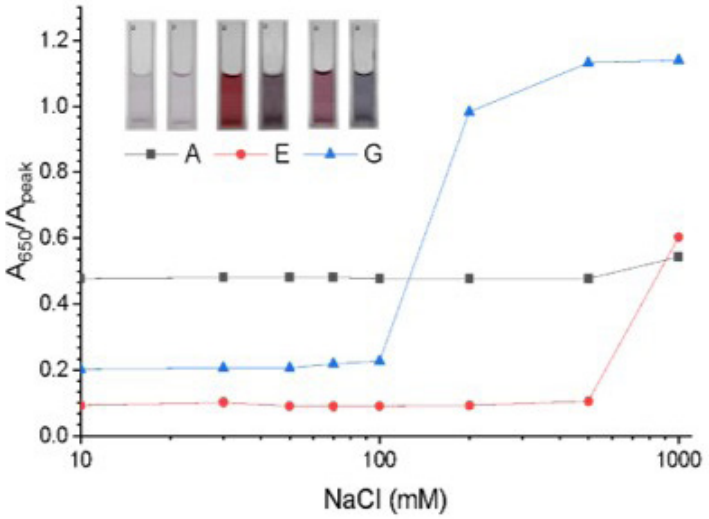

Fig. 6- UV-vis absorbance ratio of PEG-AuNPs prepared using: –■– 0.5 mM, –●– 3 mM, and –▲– 5 mM $HAuCl_4$ solution, added with various concentrations of NaCl solution. Inset images are actual samples before (left) and after (right) addition of NaCl.

agglomerate upon the addition of 200 mM NaCl as depicted by the apparent red to purple color change of the solution concurred with the sudden increase in the UV-vis absorbance ratio at 650 nm.

On the contrary, AuNPs synthesized with lower precursor concentrations exhibited stability even up to the addition of 500 mM NaCl solution. This implies that the steric repulsion between the PEG molecules adsorbed on the nanoparticle's surface provides good stability towards colloidal AuNPs dispersed in high ionic strength medium. Additionally, the stability difference of the PEG-AuNPs at different NaCl concentrations can be attributed to the role of precursor concentration in regulating the pH of the colloidal solution. Reducing the precursor concentration shifts the pH of the resulting colloids to higher values (Table 1), augmenting the electrostatic repulsion between nanoparticles due to the adsorption of OH^- ions. This strengthened repulsive interaction subsequently contributes to the stability of the colloids, leading to notably higher ionic strength thresholds compared to PEG-AuNPs obtained with relatively higher precursor concentrations. This finding underscores the enhanced colloidal stability conferred by PEG capping to AuNPs synthesized with lower precursor concentrations. It suggests that these nanoparticles possess an improved dispersion stability in the presence of salts, making them a promising candidate for in vivo and in vitro applications.

Finally, a comparison with recent studies is presented in Table 2 to contextualize the significance of our results within the existing research. Manson et al. [20] reported a commonly used method for synthesizing PEGylated AuNPs by reducing a 0.3 mM chloroauric acid precursor with trisodium citrate, followed by functionalization with PEG (Mw = 5000 g/mol). This process yielded PEG-capped AuNPs with an average particle size of 18 nm and a surface plasmon resonance (SPR) peak at 520 nm. In contrast, Leopold et al. [23] employed a more straightforward synthesis method, successfully producing PEG-reduced AuNPs via a one-step approach using a high concentration (60 mM) of $HAuCl_4$ and PEG (Mw = 200 g/mol and Mw = 8000 g/mol). This resulted in PEGylated AuNPs with sizes ranging from 15 to 60 nm and SPR peaks between 520 and 562 nm. Similarly, Stiufiuc et al. [24] synthesized spherical PEGylated AuNPs using a one-step method with 10 mM $HAuCl_4$, varying PEG molecular weights (Mw) from 200 g/mol to 20,000 g/mol, which produced average particle sizes from 10 nm to 80 nm, with corresponding SPR absorption peaks from 520 to 562 nm.

Another study by Nițică et al. [25] also utilized a one-step approach, generating 35 nm-sized PEGylated AuNPs with a maximum absorption at 530 nm using a high precursor concentration (128 mM) and PEG (Mw = 1000 g/mol). Notably, among the one-step synthesis methods reviewed, our work uniquely employs lower precursor concentrations (0.5 mM to 5 mM) and successfully produces spherical PEG-AuNPs with sizes ranging from 14.5 nm to 46.7 nm, with SPR peaks at 520 nm to 536 nm. Furthermore, this study is the first to investigate the impact of varying precursor concentrations on the physicochemical characteristics of the nanoparticles. Interestingly, we found that photoluminescence (PL) emission was highest at the lowest precursor concentration of 0.5 mM, which also demonstrated the best stability when tested under increasing NaCl concentrations.

4. Conclusion

This paper reports the viability synthesizing PEG-AuNPs via a one-step approach using reduced precursor concentrations. The morphology, optical, and structural property of the as-synthesized PEG-AuNPs were examined using TEM, DLS, FT-IR, UV-

Table 2- Comparison of PEGylated AuNPs synthesis methods between different literature studies.

PEGylated AuNPs synthesis method	$HAuCl_4$ Concentration (mM)	PEG Mw (g/mol)	Nanoparticle size (nm)	Absorption maximum (nm)	References
Citrate reduced, PEG capped AuNPs via two-step approach	~0.3	5000	18	520	[20]
PEG reduced AuNPs via One-step synthesis	~60	200 and 8000	15 - 60	520 - 562	[23]
One-step synthesized PEGylated AuNPs	10	200, 400, 1500, 4000, 6000, 10000, and 20000	10 - 80	517 - 533	[24]
PEGylated AuNPs via one-step approach	128	1000	35	530	[25]
PEG-AuNPs via one-step synthesis	0.5, 0.75, 1, 2, 3, 4, and 5	1000	14.5 - 46.7	520 - 536	This work

vis, XRD, and photoluminescence spectroscopy. The resulting colloids exhibited a well-defined absorption band, indicating the formation of nanoparticles with dominantly spherical shape as confirmed by TEM. PDI values (<0.3) reveal further that the dispersions were uniformly distributed with respect to their corresponding average hydrodynamic diameter. Notably, the precursor concentration also played a significant role in improving the stabilizing ability of PEG on AuNPs in the presence of salts, effectively preventing their aggregation even in the presence of up to 500 mM NaCl. Moreover, the fine-tuning of precursor concentration allowed for precise control over the fluorescence intensity of the synthesized AuNPs, with the most pronounced intensity observed at the lowest precursor concentration (0.5 mM). This dual achievement, marked by improved dispersion stability and tunable photoluminescence intensity, not only validates the viability of producing PEG-capped gold nanoparticles using reduced precursor concentration in one-step but also underscores the potential and versatility of the formulation and synthesis route for applications in biological sensing.

Acknowledgements

The authors acknowledged the research grant provided by Commission on Higher Education-Leading the Advancement of Knowledge in Agriculture and Sciences (CHED-LAKAS). Technical support by the Premier Research Institute in Science and Mathematics (PRISM), Center for Sustainable Polymers of MSU-Iligan Institute of Technology and the Central Instrumentation Facility of De La Salle University is also acknowledged.

Author contributions

ML: Conceptualization, investigation, validation, data curation, writing—original draft, visualization, writing—review and editing. RU: Conceptualization, investigation, validation, data curation, supervision. RLR, JO, RL, AR, and RBR: methodology, validation, data curation, writing—review and editing. AC: methodology, validation, data curation. NLS: investigation, data curation, supervision. FL: data curation, resources, supervision, writing—review and editing. RC: data interpretation, formal analysis, writing—review and editing. AHB, AL, and RM: data interpretation, formal analysis, resources. GPJ: data interpretation, formal analysis. AA: Conceptualization, investigation, validation, data curation, supervision. GD: writing—review and editing.

Funding

This work was supported by the Commission on Higher Education under the CHED-LAKAS research funding agreement 2022-003.

Declarations

The authors declare no competing interests.

References

1. Khalid K, Tan X, Mohd Zaid HF, Tao Y, Lye Chew C, Chu DT, et al. Advanced in Developmental Organic and Inorganic Nanomaterial: A Review. Bioengineered. 2020;11(1):328-355.
2. Tran CD, Prosenc F, Franko M. Facile Synthesis, Structure, Biocompatibility and Antimicrobial Property of Gold Nanoparticle Composites from Cellulose and Keratin. J Colloid Interface Sci. 2018;510:237-245.
3. Anselmo AC, Mitragotri S. Nanoparticles in the Clinic: An Update. Bioeng Transl Med. 2019;4(3).
4. Singh P, Pandit S, Mokkapati VRSS, Garg A, Ravikumar V, Mijakovic I. Gold Nanoparticles in Diagnostics and Therapeutics for Human Cancer. Int J Mol Sci. 2018;19(7):1979.
5. Kong FY, Zhang JW, Li RF, Wang ZX, Wang WJ, Wang W. Unique Roles of Gold Nanoparticles in Drug Delivery, Targeting and Imaging Applications. Molecules. 2017;22(9):1445.
6. Siddique S, Chow JCL. Gold Nanoparticles for Drug Delivery and Cancer Therapy. Appl Sci. 2020;10(11):3824.
7. Yang Z, Wang D, Zhang C, Liu H, Hao M, Kan S, et al. The Applications of Gold Nanoparticles in the Diagnosis and Treatment of Gastrointestinal Cancer. Front Oncol. 2022;11:819329.
8. Turkevich J, Stevenson PC, Hillier J. A Study of the Nucleation and Growth Processes in the Synthesis of Colloidal Gold. Discuss Faraday Soc. 1951;11:55.
9. Frens G. Controlled Nucleation for the Regulation of the Particle Size in Monodisperse Gold Suspensions. Nat Phys Sci. 1973;241(105):20-22.
10. Xin Lee K, Shameli K, Miyake M, Kuwano N, Bt Ahmad Khairudin NB, Bt Mohamad SE, et al. Green Synthesis of Gold Nanoparticles Using Aqueous Extract of Garcinia Mangostana Fruit Peels. J Nanomater. 2016;2016:1-7.
11. Zhang T, Dang M, Zhang W, Lin X. Gold Nanoparticles Synthesized from Euphorbia Fischeriana Root by Green Route Method Alleviates the Isoprenaline Hydrochloride Induced Myocardial Infarction in Rats. J Photochem Photobiol B. 2020;202:111705.
12. Rajasekar T, Karthika K, Muralitharan G, Maryshamya A, Sabarika S, Anbarasu S, et al. Green Synthesis of Gold Nanoparticles Using Extracellular Metabolites of Fish Gut Microbes and Their Antimicrobial Properties. Braz J Microbiol. 2020;51(3):957-967.
13. Chowdhury NK, Choudhury R, Gogoi B, Chang CM, Pandey RP. Microbial Synthesis of Gold Nanoparticles and Their Application. Curr Drug Targets. 2022;23(7):752-760.
14. Javed R, Sajjad A, Naz S, Sajjad H, Ao Q. Significance of Capping Agents of Colloidal Nanoparticles from the Perspective of Drug and Gene Delivery, Bioimaging, and Biosensing: An Insight. Int J Mol Sci. 2022;23(18):10521.
15. Al-Ghamdi A, Indumathi T, Ranjith Kumar E. Green Synthesized Zinc Oxide Nanoparticles: Effect of Polyethylene Glycol and Chitosan on Structural, Optical and Morphological Analysis. Ceram Int. 2022;48(13):18324-18329.
16. Javed R, Zia M, Naz S, Aisida SO, Ain NU, Ao Q. Role of Capping Agents in the Application of Nanoparticles in Biomedicine and Environmental Remediation: Recent Trends and Future Prospects. J Nanobiotechnology. 2020;18(1):172.
17. Rahme K, Dagher N. Chemistry Routes for Copolymer Synthesis Containing PEG for Targeting, Imaging, and Drug Delivery Purposes. Pharmaceutics. 2019;11(7):327.
18. Carreón González JL, García Casillas PE, Chapa González C. Gold Nanoparticles as Drug Carriers: The Role of Silica and PEG as Surface Coatings in Optimizing Drug Loading. Micromachines. 2023;14(2):451.

19. Zamora-Justo JA, Abrica-González P, Vázquez-Martínez GR, Muñoz-Diosdado A, Balderas-López JA, Ibáñez-Hernández M. Polyethylene Glycol-Coated Gold Nanoparticles as DNA and Atorvastatin Delivery Systems and Cytotoxicity Evaluation. J Nanomater. 2019;2019:1-11.
20. Manson J, Kumar D, Meenan BJ, Dixon D. Polyethylene glycol functionalized gold nanoparticles: the influence of capping density on stability in various media. Gold Bull. 2011;44:99–105.
21. López-Marzo AM, Hoyos-de-la-Torre R, Baldrich E. NaNO3/NaCl Oxidant and Polyethylene Glycol (PEG) Capped Gold Nanoparticles (AuNPs) as a Novel Green Route for AuNPs Detection in Electrochemical Biosensors. Anal Chem. 2018;90(6):4010-4018.
22. Özçiçek İ, Çakici Ç, Ayşit N, Erim ÜC. The Effects of Gold Nanoparticles with Different Surface Coatings and Sizes on Biochemical Parameters in Mice. Eur Res J. 2023;9(1):131-139.
23. Leopold N, Chiș V, Mircescu NE, Marișca OT, Buja OM, Leopold LF, et al. One Step Synthesis of SERS Active Colloidal Gold Nanoparticles by Reduction with Polyethylene Glycol. Colloids Surf Physicochem Eng Asp. 2013;436:133-138.
24. Stiufiuc R, Iacovita C, Nicoara R, Stiufiuc G, Florea A, Achim M, et al. One-Step Synthesis of PEGylated Gold Nanoparticles with Tunable Surface Charge. J Nanomater. 2013;2013:1-7.
25. Nițică Ș, Moldovan AI, Toma V, Moldovan CS, Berindan-Neagoe I, Știufiuc G, et al. PEGylated Gold Nanoparticles with Interesting Plasmonic Properties Synthesized Using an Original, Rapid, and Easy-to-Implement Procedure. J Nanomater. 2018;2018:1-7.
26. Danaei M, Dehghankhold M, Ataei S, Hasanzadeh Davarani F, Javanmard R, Dokhani A, et al. Impact of Particle Size and Polydispersity Index on the Clinical Applications of Lipidic Nanocarrier Systems. Pharmaceutics. 2018;10(2):57.
27. Sahu M, Reddy VRM, Kim B, Patro B, Park C, Kim WK, et al. Fabrication of Cu_2ZnSnS_4 Light Absorber Using a Cost-Effective Mechanochemical Method for Photovoltaic Applications. Materials. 2022;15(5):1708.
28. Dong J, Carpinone PL, Pyrgiotakis G, Demokritou P, Moudgil BM. Synthesis of Precision Gold Nanoparticles Using Turkevich Method. KONA Powder Part J. 2020;37:224-32.
29. Suárez-López R, Puntes VF, Bastús NG, Hervés C, Jaime C. Nucleation and Growth of Gold Nanoparticles in the Presence of Different Surfactants: a Dissipative Particle Dynamics Study. Sci Rep. 2022;12(1):13926.
30. Chang CH, Lin RJ, Tien CL, Yeh SM. Enhanced photoluminescence in gold nanoparticles doped homogeneous planar nematic liquid crystals. Adv Condens Matter Phys. 2018;2018:1–5.